

Online Research @ Cardiff

This is an Open Access document downloaded from ORCA, Cardiff University's institutional repository: <http://orca.cf.ac.uk/104208/>

This is the author's version of a work that was submitted to / accepted for publication.

Citation for final published version:

Dovey, Oliver M., Cooper, Jonathan L., Mupo, Annalisa, Grove, Carolyn S., Lynn, Claire, Conte, Nathalie, Andrews, Robert M., Pacharne, Suruchi, Tzelepis, Konstantinos, Vijayabaskar, M.S., Green, Paul, Rad, Roland, Arends, Mark, Wright, Penny, Yusa, Kosuke, Bradley, Allan, Varela, Ignacio and Vassiliou, George S. 2017. Molecular synergy underlies the co-occurrence patterns and phenotype of NPM1-mutant acute myeloid leukemia. *Blood* 130 (17) , pp. 1911-1922.
10.1182/blood-2017-01-760595 file

Publishers page: <http://dx.doi.org/10.1182/blood-2017-01-760595> <<http://dx.doi.org/10.1182/blood-2017-01-760595>>

Please note:

Changes made as a result of publishing processes such as copy-editing, formatting and page numbers may not be reflected in this version. For the definitive version of this publication, please refer to the published source. You are advised to consult the publisher's version if you wish to cite this paper.

This version is being made available in accordance with publisher policies. See <http://orca.cf.ac.uk/policies.html> for usage policies. Copyright and moral rights for publications made available in ORCA are retained by the copyright holders.



Dovey et al

MOLECULAR SYNERGY IN *NPM1* MUTANT AML

Molecular synergy underlies the co-occurrence patterns and phenotype of *NPM1*-mutant acute myeloid leukemia.

Oliver M Dovey¹, Jonathan L Cooper¹, Annalisa Mupo¹, Carolyn S Grove^{1,3,4}, Claire Lynn⁵, , Nathalie Conte⁶, Robert M Andrews⁷, Suruchi Pacharne¹, Konstantinos Tzelepis¹, MS Vijayabaskar¹, Paul Green¹, Roland Rad⁸, Mark Arends⁹, Penny Wright², Kosuke Yusa¹, Allan Bradley¹, Ignacio Varela¹⁰, and George S Vassiliou^{1-2†}.

¹The Wellcome Trust Sanger Institute, Wellcome Trust Genome Campus, CB10 1SD, United Kingdom.

²Department of Haematology, Cambridge University Hospitals NHS Trust, Cambridge, UK.

³School of Pathology and Laboratory Medicine, University of Western Australia, Crawley, Western Australia, Australia.

⁴PathWest Division of Clinical Pathology, Queen Elizabeth II Medical Centre, Nedlands, Western Australia, Australia.

⁵Leukemia and Stem Cell Biology Group, Division of Cancer Studies, Department of Haematological Medicine, King's College London, Denmark Hill Campus, London SE5 9NU, UK.

⁶Sample Phenotype Ontology Team, The European Bioinformatics Institute, Wellcome Trust Genome Campus, CB10 1SD, United Kingdom.

⁷Institute of Translation, Innovation, Methodology and Engagement, Cardiff University School of Medicine, Heath Park, Cardiff, UK.

⁸Department of Medicine II, Klinikum Rechts der Isar, Technische Universität München, 81675 Munich, Germany; German Cancer Consortium (DKTK), German Cancer Research Center (DKFZ), 69120 Heidelberg, Germany.

⁹Cancer Research UK Edinburgh Centre, Institute of Genetics and Molecular Medicine, University of Edinburgh, Crewe Road, Edinburgh, UK.

¹⁰Instituto de Biomedicina y Biotecnología de Cantabria, Santander 39011, Spain.

†Correspondence: gsv20@sanger.ac.uk

Running Title: Molecular synergy in *NPM1* mutant AML

Include article word count here: 3966

Abstract Word Count: 247

Scientific Category: Myeloid Neoplasia

Number of figures: 6

Number of references: 39

32 **Key Points**

33 *Npm1c* and *Nras-G12D* co-mutation in mice leads to AML with a longer latency and a more
34 mature phenotype than the *Npm1c/Flt3-ITD* combination

35 Mutant *Flt3* or *Nras* allele amplification is the dominant mode of progression in *Npm1c/Flt3-*
36 *ITD* and *Npm1c/Nras-G12D* murine AML

Abstract

NPM1 mutations define the commonest subgroup of acute myeloid leukemia (AML) and frequently co-occur with *FLT3* internal tandem duplications (ITD) or, less commonly, *NRAS* or *KRAS* mutations. Co-occurrence of mutant *NPM1* with *FLT3*-ITD carries a significantly worse prognosis than *NPM1*-RAS combinations. To understand the molecular basis of these observations we compare the effects of the two combinations on hematopoiesis and leukemogenesis in knock-in mice. Early effects of these mutations on hematopoiesis show that compound *Npm1*^{cA/+};*Nras*^{G12D/+} or *Npm1*^{cA};*Flt3*^{ITD} share a number of features: *Hox* gene over-expression, enhanced self-renewal, expansion of hematopoietic progenitors and myeloid differentiation bias. However, *Npm1*^{cA};*Flt3*^{ITD} mutants, displayed significantly higher peripheral leucocyte counts, early depletion of common lymphoid progenitors and a monocytic bias compared to the granulocytic bias in *Npm1*^{cA/+};*Nras*^{G12D/+} mutants. Underlying this was a striking molecular synergy manifested as a dramatically altered gene expression profile in *Npm1*^{cA};*Flt3*^{ITD}, but not *Npm1*^{cA/+};*Nras*^{G12D/+}, progenitors compared to wild type. Both double-mutant models developed high penetrance AML although latency was significantly longer with *Npm1*^{cA/+};*Nras*^{G12D/+}. During AML evolution, both models acquired additional copies of the mutant *Flt3* or *Nras* alleles, but only *Npm1*^{cA/+};*Nras*^{G12D/+} mice showed acquisition of other human AML mutations, including *IDH1* R132Q. We also find, using primary Cas9-expressing AMLs, that *HoxA* genes and selected interactors or downstream targets are required for survival of both types of double-mutant AML. Our results show that molecular complementarity underlies the higher frequency and significantly worse prognosis associated with *NPM1c/FLT3-ITD* versus *NPM1/NRAS-G12D*-mutant AML and functionally confirm the role of *HOXA* genes in *NPM1*-driven AML.

[247 words]

Introduction

Advances in genomics have defined the somatic mutational landscape of acute myeloid leukemia (AML), leading to a detailed characterisation of their prognostic significance and patterns of mutual co-occurrence or exclusivity.^{1,2} Mutations in *NPM1*, the gene for Nucleophosmin, characterise the most common subgroup of AML representing 25-30% of all cases, result in cytoplasmic dislocation of the protein (*NPM1c*) and are mutually exclusive of leukemogenic fusion genes.¹⁻³ As is often the case for fusion genes, progression to AML after the acquisition of mutant *NPM1* is contingent upon the gain of additional somatic mutations such as those that activate STAT and/or RAS signalling^{3,4}. For reasons that are not clear, this transforming step favours acquisition of internal tandem duplications in *FLT3* (*FLT3-ITD*) over other somatic mutations with similar effects such as those involving *NRAS* or *KRAS*.¹⁻⁴ Furthermore, the *NPM1c/FLT3-ITD* combination is associated with a significantly worse prognosis compared to combinations of *NPM1c* with mutant *NRAS*, *KRAS* or other mutations.²

Whilst the adverse prognostic impact of *NPM1/FLT3-ITD* vs *NPM1/RAS* co-mutation influences clinical decisions in AML, its molecular basis and that of the frequent co-occurrence of *NPM1c* and *FLT3-ITD* in AML are unknown. Here, in order to investigate these phenomena, we compare the interaction of *Npm1c* with *Flt3-ITD* to its interaction with *Nras*^{G12D} in knock-in mice. Individually, knock-in models of *NPM1c*, *FLT3-ITD* and *NRAS-G12D* display enhanced myelopoiesis and progression to myeloproliferative disorders or AML in a significant proportion of animals.⁵⁻⁷ Also, we and others have previously shown that *Npm1c* and *Flt3-ITD* synergise to drive rapid-onset AML^{8,9}, but the interaction between *Npm1c* and mutant *Nras*^{G12D} has not, to our knowledge, been previously investigated in knock-in mice¹⁰. Our findings reveal that the combination of *Npm1c* and *Flt3-ITD* has an early profound effect on gene expression and hematopoiesis, whilst *Npm1c* and *Nras-G12D* display only modest molecular synergy and subtler cellular changes. Also, whilst both types of co-mutation drove AML in the majority of mice, the leukemias in *Npm1c;Flt3-ITD* mice were more aggressive and undifferentiated than those which developed in *Npm1c;Nras-G12D* animals. At the genomic level, there was frequent amplification in both models of the mutant *Flt3-ITD* or *Nras-G12D* allele, however additional somatic mutations in AML driver genes (e.g. *Idh1* and *Ptpn11*) were seen only in *Npm1c;Nras-G12D* AMLs. Our findings propose that the molecular synergy between *Npm1c* and *Flt3-ITD* underpin the co-occurrence patterns, phenotype and prognosis of *NPM1*-mutant AML.

97 **Materials and methods**

98 **Animal husbandry**

99 *Mx1-Cre⁺;Npm1^{flox-cA/+}* were crossed with *Nras^{LSL-G12D}* or *Flt3^{ITD}* mice, to generate triple transgenic
100 animals (*Mx1-Cre;Npm1^{flox-cA/+};Nras^{LSL-G12D/+}* and *Mx1-Cre;Npm1^{flox-cA/+};Flt3^{ITD/+}*). To activate
101 conditional alleles (*Npm1^{cA}* and *Nras^{G12D}*) in approximately 12-14 week old *Mx1-Cre;Npm1^{flox-}*
102 *cA/+;Nras^{LSL-G12D/+}* mice, *Mx1-Cre* was induced by administration of plpC. As described previously, *Mx-1*
103 *Cre;Npm1^{flox-cA/+};Flt3^{ITD/+}* mutants do not require plpC induction of *Mx1-Cre* and recombination of the
104 *Npm1^{flox-cA}* allele.⁸ For pre-leukemic analyses *Npm1^{cA/+};Nras^{G12D/+}* were sacrificed 4-5 weeks post plpC
105 and *Npm1^{cA/+};Flt3^{ITD/+}* were sacrificed at 5 weeks of age. Genotyping for mutant alleles was
106 performed as previously described.⁵⁻⁷ All animal procedures were carried out in accordance with the
107 Home Office Animals (Scientific Procedures) Act 1986 Amendment Regulations (2012) under project
108 license 80/2564.

109 **Hematological measurements**

110 Blood counts were performed on a VetABC analyzer (Horiba ABX).

111 **Histopathology**

112 Formalin fixed, paraffin embedded (FFPE) sections were stained with hematoxylin and eosin.
113 Samples from leukemic mice were also stained with anti-CD3, anti-B220 and anti-myeloperoxidase.
114 All material was examined by two experienced histopathologists (P.W. and M.A.) blinded to mouse
115 genotypes.

116 **Colony-forming assays and serial re-plating**

117 Nucleated cells (3×10^4) from bone marrow (BM) aspirates of mutant and wild-type mice were
118 suspended in cytokine-containing methylcellulose-based media (M3434, Stem Cell Technologies)
119 and plated in duplicate wells of 6-well plates. Colony-forming units (CFUs) were counted 7 days later.
120 For serial re-plating, 3×10^4 cells were re-seeded and colonies counted after 7 days.

121 **Flow cytometry and cell sorting**

122 Single cell suspensions of BM cells or splenocytes were incubated in 0.85% NH_4Cl for 5 minutes to
123 lyse erythrocytes. Cells were then suspended in Hank's Balanced Salt Solution (HBSS) supplemented
124 with 2% FCS and 10 μM HEPES. Progenitor populations were defined and stained as described in

supplementary methods. Gated cellularity was calculated by multiplying the percentage of gated cells by the total number of nucleated cells from BM samples after erythrocyte depletion.

Viral transduction of BM progenitors and AML cell culture.

Lineage depleted BM aspirates, isolated from wildtype and *Flt3^{ITD/+}* mice, were transduced with MSCV-*Hoxa9*-GFP and/or MSCV-*Nkx2-3*-CFP retroviruses and expanded for 7 days in liquid culture (X-Vivo, Lonza, supplemented with 10ng/ml IL-3, 10ng/ml IL-6 and 50ng/ml SCF, Peprotech). CFP, GFP or double positive cells were FACS sorted and 2.5×10^4 cells re-plated in semi-solid media as previously described. BM-derived AML cells from Roas26-EF1-Cas9 mice were cultured *in vitro* in the presence of cytokines. Disruption of individual candidate genes was performed by transduction with lentivirus expressing gene-specific guide RNA (gRNA) and blue fluorescent protein (BFP). The impact of gene disruption on AML cell growth was determined using competitive co-culture of transduced (BFP+) vs non-transduced (BFP-) cells as described previously¹¹ (Figure 6A, Supplemental methods).

Microarray and comparative genomic hybridization analysis

Mouse gene expression profiles (GEPs) were generated using the Illumina MouseWG-6 v2 Expression BeadChip platform (Illumina). DNA copy number variation in leukemic samples was assessed with Mouse Genome Comparative Genomic Hybridization 244K Microarray (acGH, Agilent Technologies). Full details of analysis are provided in supplemental methods. For mouse gene expression profiling, n=4-10 (Lin⁻) or n=3-5 (MPP).

AML exome sequencing and mutation calling

Whole exome sequencing (WES) of AML BM and control C57BL/6N or 129Sv tail DNA was performed using the Agilent SureSelect Mouse Exon Kit (Agilent Technologies) and paired-end sequencing on a HiSeq2000 sequencer (Illumina). Validation of mutations was performed using MiSeq sequencing (Illumina) of amplicon libraries as previously described (See Supplemental Methods Figure S1 and Supplemental Tables 6 and 7 for primer sequences).^{12,13} Full details of analysis are provided in supplemental methods.

Datasets

Microarray data were deposited at Array Express (accession number E-MTAB-5356), and RNA sequencing (accession numbers ERS1732539 to ERS1732546, ERS812461 and ERS812462) as well as exome and Miseq sequencing (accession numbers PRJEB18526 and ERP020464) at EBI ENA.

Dovey et al

MOLECULAR SYNERGY IN *NPM1* MUTANT AML

155

Results

Mutant *Npm1* co-operates with *Nras-G12D* and *Flt3-ITD* to increase self-renewal of hematopoietic progenitors and expand myelopoiesis

To understand the impact of the studied mutations, we analyzed hematopoietic cell compartments of *Npm1*^{cA/+};*Nras*^{G12D/+}, *Npm1*^{cA/+};*Flt3*^{ITD/+}, *Nras*^{G12D/+}, *Flt3*^{ITD/+} and wild type (WT) mice 4-6 weeks after activation of conditional mutations (Figure 1). Compared to *Flt3*^{ITD/+} single mutants, *Npm1*^{cA/+};*Flt3*^{ITD/+} mice displayed higher white cell counts (WCC) (56±13.4 vs 6.5±0.5 x10⁶ g/L, p<0.001) and spleen weights (0.63g vs 0.16g, p<0.001), but not BM cellularity (Figure 1B). By contrast, both *Nras*^{G12D/+} and *Npm1*^{cA/+};*Nras*^{G12D/+} mutants exhibited subtler increases in spleen weight (WT: 0.12g, *Nras*^{G12D/+}: 0.18g, *Npm1*^{cA/+};*Nras*^{G12D/+}: 0.19g, p<0.01 and p<0.001 respectively), but increased BM cellularity (WT: 28.1±1.9 x10⁶, *Nras*^{G12D/+}: 43.7±2.6 x 10⁶ and *Npm1*^{cA/+};*Nras*^{G12D/+}: 41.3±3.2 x10⁶, p<0.01 for either comparison vs WT) (Figure 1B).

Expanded myelopoiesis and myeloproliferation were previously documented in single *Nras*^{G12D/+} and *Flt3*^{ITD/+} mutant mice.^{5,6} Mutant *Npm1* augmented these phenotypes with increases in total Mac-1⁺ splenocytes (from 27% to 50% for *Nras*^{G12D/+}; and 57% to 73% for *Flt3*^{ITD/+}). Notably, these cells were predominantly granulocytic (Mac-1⁺/Gr-1⁺) in *Npm1*^{cA/+};*Nras*^{G12D/+} and predominantly monocytic (Mac-1⁺/Gr-1⁻) in *Npm1*^{cA/+};*Flt3*^{ITD/+} mice (Supplemental Figure S1A).

Nras^{G12D/+} mice have been shown to have increased hematopoietic stem (HSC) and progenitor cell numbers, due to increased proliferation and self-renewal of the HSC and multipotent progenitor (MPP) compartments.^{14,15} Our results confirm these data demonstrating significant increases in total myeloid progenitors i.e. granulocyte-macrophage (GMP) and common-myeloid progenitors (CMP). Total numbers of Sca-1/Kit positive early progenitors (LSK) and MPPs are also increased in both *Npm1*^{cA/+};*Nras*^{G12D/+} and *Nras*^{G12D/+} BM cells (Figure 1C and Supplemental Figure S2A). However, *Nras*^{G12D/+} progenitor cell composition was largely unaltered by the addition of mutant NPM1. Concordant with previous studies, hematopoiesis in *Flt3*^{ITD/+} mice was characterised by increased numbers of total myeloid progenitors (LK p<0.05 and GMPs p<0.01) and early progenitor populations (LSK, MPP and LMPP, p<0.01, p<0.01 and p<0.05 respectively) (Figure 1C and Supplemental Figure S2A).^{16,17} Of note, there were detectable decreases in the size of the common lymphoid progenitor (CLP) population in *Flt3*^{ITD/+} and *Npm1*^{cA/+};*Flt3*^{ITD/+} mice (Figure 1C) (in part due to the reduction in Il-7Rα-positive cells) (Figure S2B). *Npm1*^{cA/+};*Flt3*^{ITD/+} mice also exhibited robust increases in numbers of LK, LSK, MPP and LMPP populations, above what was observed with *Flt3*^{ITD/+}, when compared to WT. In direct comparison with *Flt3*^{ITD/+} mutants, numbers of CMP and MEP

progenitors in *Npm1*^{cA/+}; *Flt3*^{ITD/+} mice were reduced (from 55x10³ to 16x10³, p<0.05 and from 61x10³ to 17x10³, p<0.05), yet GMPs, proposed as direct descendants of CMPs¹⁸, are significantly increased. This demonstrates that *Flt3*^{ITD/+} mutant myelopoiesis is dramatically altered by the addition of *Npm1*^{cA/+}. In direct comparison with *Npm1*^{cA/+}; *Nras*^{G12D/+}, *Npm1*^{cA/+}; *Flt3*^{ITD/+} mice showed increased LMPP and GMP populations with reduced numbers of lymphoid progenitors (CLP) (Figure 1E).

In order to assess the effects on the earliest detectable hematopoietic stem cell compartment (HSC) we opted to perform E-SLAM staining (CD45⁺/EPCR⁺/CD48⁻/CD150⁺).¹⁹ Importantly, this does not rely on cell surface expression of FLT3, and reveals the percentage of E-SLAM detectable HSCs is decreased in *Npm1*^{cA/+}; *Nras*^{G12D/+} mice and further so in *Npm1*^{cA/+}; *Flt3*^{ITD/+} mutants (Figure 1D). Finally, using serial re-plating of BM cells in semi-solid media we show that *Npm1*^{cA/+} co-mutation markedly increased self-renewal of *Flt3*^{ITD/+} (as shown previously⁸) and of *Nras*^{G12D/+} cells (Figure 1F).

An *Npm1*^{cA/+} transcriptional signature persists in double mutant hematopoietic progenitors

To examine their combined effects on transcription we performed comparative global gene expression profiling of lineage negative (Lin⁻) BM cells using microarrays. *Npm1*^{cA/+}; *Nras*^{G12D/+} and *Npm1*^{cA/+}; *Flt3*^{ITD/+} cells displayed a dramatically altered GEP compared to single *Nras*^{G12D/+} or *Flt3*^{ITD/+} mutants (Figure 2A and Supplemental Figure S3B). Previously, we showed that mouse *Npm1*^{cA/+} Lin⁻ cells overexpressed several homeobox (*Hox*) genes (in particular overexpression of *Hoxa5*, *Hoxa7*, *Hxa9* and two other homeobox genes, *Hopx* and *Nkx2-3*).⁷ Here, we show that this signature, absent from *Nras*^{G12D/+} or *Flt3*^{ITD/+} singular mutant mice, persists in compound *Npm1*^{cA/+}; *Nras*^{G12D/+} and *Npm1*^{cA/+}; *Flt3*^{ITD/+} Lin⁻ progenitors. (Figure 2A, Supplemental Figure S3A-C). Gene Set Enrichment Analysis (GSEA) of *Npm1*^{cA/+} single and compound mutant cell GEPs, showed significant enrichment for genes up-regulated in NPM1-mutant and *MLL*-fusion gene positive human leukemias (Figure 2A).

Overexpression of the homeobox gene NKX2.3 in human NPM1-mutant AML

Using the human TCGA AML dataset, we compared GEPs of NPM1 mutant (NPM1c^{+ve}) to NPM1 wildtype (NPM1^{wt}) AML.¹ In agreement with previously published analyses, both *HOXA* and *HOXB* genes were significantly overexpressed in NPM1c^{+ve} AML (Figure 2B).²⁰ We also noted *NKX2-3* was also overexpressed in keeping with our findings in *Npm1*^{cA/+} mice (Figure 2A). Recently, *NKX2-3* overexpression was shown to be the most effective discriminant of *MLL-MLLT4* (*MLL-AF6*)-driven AML from AMLs driven by other *MLL*-fusion genes.²¹ Whilst overexpression of *Hox* genes such as *Hoxa9* has been shown to impart increased self-renewal and proliferation of hematopoietic progenitors, the effects of *Nkx2-3* overexpression are unknown.²² To study this we performed retroviral gene transfer of fluorescently tagged *Nkx2-3*-CFP and *Hoxa9*-GFP into wildtype and *Flt3*^{ITD/+}

Lin⁻ cells. Cells were subsequently sorted and plated in semi-solid methylcellulose for colony formation assays (Figure 2Ci). We find that overexpression of *Nkx2-3* increases clonogenic potential, albeit to a lesser extent compared to *Hoxa9* overexpression, in both wildtype and *Flt3*^{ITD/+} progenitors. Notably, this is not augmented in combined transfected cells. (Figure 2Cii).

***Hoxa* gene expression is unaltered in mutant *NPM1* early multipotent progenitors**

In order to mitigate the impact of the studied driver mutations on cell surface phenotypes, we performed transcriptome analysis on a homogeneous population of early progenitors, purified LSK-MPPs, (Figure 2D). *Hox* gene expression was not significantly altered in this population in any of the *Npm1*^{cA/+} models when compared to wildtype or single *Nras*^{G12D/+} and *Flt3*^{ITD/+} mutants (Figure 2E and Figure S3C). These results are in agreement with observations that *Hox* gene expression in human NPM1c AML blasts is comparable to that seen in WT human HSCs and myeloid progenitors.²⁰ As we do not observe statistically significant expansion in total (Lin⁻) progenitors in single *Npm1*^{cA/+} mice (figure 1C), these data propose that, unlike HSCs, the observed pattern of *Hox* overexpression in these progenitors is a molecular consequence of NPM1c rather than a change in cellular composition. This concurs with our published observations that the *Hox* signature is detectable even in CD19-positive B-cells⁷.

MPPs from single *Nras*^{G12D/+} or *Flt3*^{ITD/+} and the respective *Npm1*^{cA/+} compound mutant MPPs also had distinct transcriptional changes. Compared to WT, both *Nras*^{G12D/+} and *Npm1*^{cA/+}; *Nras*^{G12D/+} MPPs displayed small numbers of differentially expressed genes yet only ~20% of these were shared (Figure 2Di). GSEA did not uncover significant overlap with any pre-established expression signatures (data not shown). In contrast, the “addition” of *Npm1*^{cA/+} to *Flt3*^{ITD/+} in MPPs led to differential expression of a large number of additional genes, whilst also retaining most of the transcriptional changes attributable to *Flt3*^{ITD/+} (Figure 2Dii, Table S2) demonstrating the powerful synergy between *Npm1*^{cA/+} and *Flt3*^{ITD/+}. Pathway analysis of genes differentially expressed in *Npm1*^{cA/+}; *Flt3*^{ITD/+} MPPs revealed enrichment of genes in the JAK-STAT pathway (Supplemental Figure 3E, Supplemental Tables S4), including the negative regulators *Cish* and *Socs2* (Figure 2F). A number genes, encoding proteins involved in MAPK signaling were also deregulated, as were genes involved in chromatin regulation/organisation and hematopoietic/myeloid differentiation (Figure 2F, Supplemental Figure 3D). Many of the genes in our *Npm1*^{cA/+}; *Flt3*^{ITD/+} dataset were also found deregulated in a recently published Tet2^{-/-}; *Flt3*^{ITD/+} mouse model of AML (, Supplemental Figure 3F and Supplemental Table 6,) which serves to verify our mouse dataset technically, but also reveals a distinguishing expression signature of FLT3-ITD which includes *Socs2*, *Id1*, *Csfr3r* and *Bcl11a*.¹⁷ In contrast a lack of correlation

between deregulated gene sets of *Npm1*^{cA/+};*Flt3*^{ITD/+} and *Npm1*^{cA/+};*Nras*^{G12D/+} MPPs (Supplemental Figure S3D) emphasises the molecular distinction between these compound mutants.

***Npm1*^{cA/+} and *Nras*^{G12D} collaborate to promote high penetrance AML**

To understand the leukemogenic potential of combined *Npm1*^{cA/+} and *Nras*^{G12D} mutations, we aged combined and single mutant cohorts. Compound *Npm1*^{cA/+};*Nras*^{G12D/+} and *Npm1*^{cA/+};*Flt3*^{ITD/+} mice had significantly reduced survival (median 138 and 52.5 days respectively) when compared to wildtype (618 days), *Npm1*^{cA/+} (427 days), *Nras*^{G12D/+} (315 days) and *Flt3*^{ITD/+} (also 315 days) (Figure 3A, Supplemental Figure S4A). No difference in the survival of *Nras*^{G12D/+} and *Flt3*^{ITD/+} mutant mice was observed (p=0.85, see Supplemental Figure S4A for all comparisons). At time of sacrifice, blood counts and tissues were collected and subjected to histopathological analysis. Aged *Npm1*^{cA/+};*Nras*^{G12D/+} and *Npm1*^{cA/+};*Flt3*^{ITD/+} mice exhibited characteristic AML pathological findings at a much higher frequency than single mutant mice. These included significantly higher WCC, reduced platelet numbers and substantial organ infiltration with leukemic cells (Supplemental Figure S4B-D). Histological analysis verified the increased AML incidence from 41% (*Flt3*^{ITD/+}) to 100% in *Npm1*^{cA/+};*Flt3*^{ITD/+} samples and from 13% (*Nras*^{G12D/+}) to 85% in *Npm1*^{cA/+};*Nras*^{G12D/+} samples (45% AML with maturation, AML⁺ and 40% AML without maturation, AML⁻ as defined by the Bethesda classification²³ (Figure 3B).

Additional somatic mutations are required for progression to AML in *Npm1*^{cA/+};*Nras*^{G12D/+} mice.

Npm1^{cA/+};*Flt3*^{ITD/+} mice succumb to AML significantly more rapidly, compared to *Npm1*^{cA/+} and *Npm1*^{cA/+};*Nras*^{G12D/+} mice. We hypothesised that the slower onset of AML in the latter two genotypes may be due to the requirement for additional cooperating mutations. To test this, we performed aCGH and WES of AMLs from *Npm1*^{cA/+}, *Npm1*^{cA/+};*Flt3*^{ITD/+} and *Npm1*^{cA/+};*Nras*^{G12D/+} mice. We first confirmed the frequent development of loss-of-heterozygosity (LOH) at the *Flt3* locus in *Npm1*^{cA/+};*Flt3*^{ITD/+} AMLs^{8,24} and verified this by quantifying *Flt3*^{ITD} variant allele fractions (VAFs) using PCR-MiSeq (Figure 4Ai). aCGH showed that LOH was copy-neutral and due to uniparental disomy of *Flt3*^{ITD} (Supplementary Figure 4Aii). Interestingly, aCGH of *Npm1*^{cA/+};*Nras*^{G12D/+} samples revealed amplification of chr3 in 5/10 samples tested (Figure 4Bi). This was exclusive to *Npm1*^{cA/+};*Nras*^{G12D/+} AMLs and mapped to a minimally amplified region (chr3: 102743581-103470550) containing *Nras* (Supplementary Table S10). We confirmed these *Nras*^{G12D} copy gains using PCR-MiSeq and also found copy neutral LOH for *Nras*^{G12D} in 3/10 AMLs. In addition, we found copy neutral LOH in 3 of 4 *Npm1*^{cA/+};*Nras*^{G12D/+} AMLs not studied by aCGH. In summary, increased *Nras*^{G12D} dosage was detected

in 11/14 *Npm1*^{cA/+};*Nras*^{G12D/+} AMLs (Figure 4Bii), and this correlated with levels of RAS pathway activation as measured by pERK1/2 staining (Figure 4C).

WES revealed that the average number of single nucleotide variants (SNVs) and small insertions/deletions (indels) per AML sample correlated positively to survival (Figure 5A). *Npm1*^{cA/+} AMLs spontaneously acquired mutations in genes involved in RAS signaling (*Nras*-p.Q61H, *Cbl*-p.S374F, *Ptpn11*-p.S502L, *Nf1*-p.W1260* and *Nf1*-R683*) confirming this genetic interaction. Likewise, we detected a spontaneous tyrosine kinase domain mutation in *Flt3*, (*Flt3*-p.D842G) confirming the importance of FLT3 mutations in progression of NPM1-mutant AML (Figure 5B-C, Supplemental Table 9). Interestingly, a single *Npm1*^{cA/+};*Nras*^{G12D/+} AML harbored an *Idh1*-p.R132Q mutation and mirroring the R132H/R132C mutations commonly seen in human AML¹ whilst IDH1-R132Q itself was reported in human chondrosarcoma.²⁵ aCGH also revealed complete or partial gain of a minimally amplified region on chr7 in 7/8 *Npm1*^{cA/+} and 4/9 *Npm1*^{cA/+};*Nras*^{G12D/+} AMLs containing genes implicated in leukemogenesis including *Nup98*, *Wee1* and *Eed*, (Supplemental Figure S5C).^{7,26-28} Single copy loss of a region containing the epigenetic modifiers *Wt1*, *Asxl1*, *Dnmt3a* (1/8 *Npm1*^{cA/+}) and a focal deletion of *Ezh2* (1/9 *Npm1*^{cA/+}; *Nras*^{G12D/+}) were also detected (Figure 5C and Supplemental Figure S5C).

***MLL*, *Hox* genes and their partners are required for the survival of *Npm1*^{cA}-driven AML cells.**

To assess their contribution to AML maintenance in *Npm1*^{cA/+};*Nras*^{G12D/+} and *Npm1*^{cA};*Flt3*^{ITD} mice, we employed CRISPR-Cas9 to disrupt selected deregulated genes identified by our pre-leukemic GEP, studies. For this, we bred with *Rosa26-EF1-Cas9* animals¹¹ to generate *Rosa26*^{Cas9/+};*Npm1*^{cA/+};*Nras*^{G12D/+}; and *Rosa26*^{Cas9/+};*Npm1*^{cA/+};*Flt3*^{ITD/+} mice. Competitive co-culture of gRNA transduced and non-transduced BM cells from these mice revealed that *Hoxa10* and to a lesser degree *Hoxa9*, but not *Hoxa7* are required for *Npm1*^{cA/+};*Nras*^{G12D/+} and *Npm1*^{cA};*Flt3*^{ITD/+} AML maintenance (Figure 6B). In contrast, all three *HoxA* genes were required for growth of AMLs generated by retroviral *MLL-AF9* transformation of *Flt3*^{ITD/+} BM cells (Supplementary Figure S7C).^{11,29,30} Notably, although *Nkx2-3* overexpression enhanced colony-forming ability of wild type and *Flt3*^{ITD/+} BM (Figure 2C), disruption of endogenous *Nkx2-3* did not significantly affect proliferation of *Npm1*^{cA/+};*Nras*^{G12D/+} or *Npm1*^{cA};*Flt3*^{ITD/+} AMLs *in vitro*. Other genes whose disruption reduced proliferation of *Npm1*^{cA}-driven AMLs included *Mll* (*Kmt2a*) gene, recently shown to be a therapeutic target in this AML type³¹, *Hoxa9/10* partners or co-factors including *Meis1*, *Pbx1* and *Pbx3*, the *HOXA9* targets *Bcl2* and *Lmo2*³²⁻³⁴. A number of genes with altered expression in mutant pre-leukemic MPP cells, were not required for survival of AML cells *in vitro* (Figure 6C). However, we cannot exclude a potential role for these in leukemia initiation.

We also wanted to investigate potential differences in JAK/STAT vs RAS signaling in our AMLs in a similar way. *FLT3-ITD* leads to constitutive activation of JAK/STAT signaling, driving growth and

transformation of hematopoietic cells³⁵⁻³⁷. In keeping with this, our transcriptome analysis revealed that genes involved in JAK/STAT signaling (*Stat5a*, *Cish*, *Socs2*) were differentially expressed in *Npm1*^{cA};*Flt3*^{ITD} but not in *Npm1*^{cA};*Nras*^{G12D} Lin⁻ progenitors. Nevertheless, CRISPR-targeting of *Jak2* and *Stat5a/b* genes inhibited the growth of both *Npm1*^{cA};*Flt3*^{ITD/+} and *Npm1*^{cA/+};*Nras*^{G12D/+} AML cells (Supplemental Figure S8B). We confirmed by RNA-seq that this was due to activation of a JAK/STAT programme in *Npm1*^{cA/+};*Nras*^{G12D/+} AML cells (Figure S9). In this light we conclude that the cytokines required for culturing primary AML cells in vitro (IL-3, IL-6 and SCF), precludes the assessment of signaling genes in AML growth and proliferation.

Discussion

Whilst the mutational drivers of AML and their patterns of co-occurrence are well understood, the molecular basis for the frequency and prognostic impact of these patterns remain unknown. Of particular clinical relevance are the co-occurrence patterns of mutant *NPM1* mutations, which characterize the most common AML subtype^{1,2}. Co-mutation of *NPM1* with *FLT3-ITD* is both significantly more frequent and carries a worse prognosis than co-mutation with *RAS genes*.^{1,2} To understand the basis of this observation we investigated the interactions of these mutations in bespoke experimental models (Figure 1A). Analysis of the short-term impact of these mutations on hematopoiesis confirmed that single *Npm1*^{cA/+} mutant mice have normal BM cellularity, WCC and splenic weight.⁷ As described before, single *Flt3*^{ITD/+} and *Nras*^{G12D/+} had moderate but significant increases in splenic size, whilst *Nras*^{G12D/+} had raised WCC and BM cellularity.^{5,6} Introduction of *Npm1*^{cA/+} into the *Nras*^{G12D/+} background did not alter these parameters significantly, yet the *Npm1*^{cA/+};*Flt3*^{ITD/+} co-mutation led to a dramatic rise in WCC and splenic size (Figure 1B). At the cellular level, the *Npm1*^{cA/+};*Nras*^{G12D/+} combination did not change progenitor and stem cell numbers when compared to *Nras*^{G12D/+} alone. In contrast, when compared to *Flt3*^{ITD/+} mutants, *Npm1*^{cA/+};*Flt3*^{ITD/+} mice displayed reductions in CMP and MEP, and increases in LSK progenitors. Furthermore, *Npm1*^{cA/+};*Flt3*^{ITD/+} mice showed a profound reduction in phenotypic HSCs (Figure 1 C–E).

The differential impact of *Npm1*^{cA/+} on *Flt3*^{ITD/+} versus *Nras*^{G12D/+} was reflected in marked differences in GEPs between double mutant mice. The *Npm1*^{cA/+};*Nras*^{G12D/+} model displayed only minimal differences to single *Nras*^{G12D/+}, whilst *Npm1*^{cA/+};*Flt3*^{ITD/+} Lin⁻ progenitors had profoundly different GEPs to *Flt3*^{ITD/+}. From these and complimentary analyses of human *NPM1c* AML we identify *NKX2-3* as a marker of this type of AML. Expression of *NKX2-3* distinguishes *MLL-AF6* and *MLL-ENL* from other forms of *MLL*-mutant leukemia^{21,38}, highlighting the mechanistic links between *NPM1c*- and *MLL*-fusion genes. Here, we show that whilst potent overexpression of *Nkx2.3* by lentivirus may have

an impact on self-renewal, genetic disruption of the endogenous *Nkx2.3* did not inhibit AML cell growth (Figure 6).

We went on to age double mutant mice and report that, like *Npm1*^{cA/+};*Flt3*^{ITD/+} animals, *Npm1*^{cA/+};*Nras*^{G12D/+} mice also develop highly penetrant AML, albeit with a much longer latency and a more mature phenotype overall. Interestingly single mutant *Flt3*^{ITD/+} and *Nras*^{G12D/+} mice had similar survival (Figure 3A), indicating that the interaction with *Npm1*^{cA} was central to this difference. To understand the genetic events involved in leukemic progression, we performed exome sequencing and copy number analysis of *Npm1*^{cA/+};*Flt3*^{ITD/+} and *Npm1*^{cA/+};*Nras*^{G12D/+} AMLs. Interestingly, the commonest somatic event during AML progression was an increase in *Nras*^{G12D/+} or *Flt3*^{ITD/+} mutant allele burden, through copy-neutral LOH or copy number gain. In human AML, copy-neutral LOH is common for *FLT3-ITD*, but less so for mutant *NRAS*; for example in a recent study we identified only one such LOH event amongst 13 *RAS* mutant human AMLs.¹³ Nevertheless, in keeping with our findings, studies using the *Nras*^{G12D/+} model, in combination with retroviral insertional mutagenesis, resulted in high penetrance AML with frequent LOH for *Nras-G12D* when combined with overexpression of oncogenes such as *Evi1*.^{6,39} The different incidence of LOH for mutant *RAS* between murine and human AML may operate through the fact that, compared to the acquisition of other oncogenic mutations (e.g. *Idh1*-R132Q in our study), LOH for *Nras-G12D* may be more expedient in mice given the large numbers of *Npm1*^{cA/+}/*Nras*^{G12D/+} pre-leukemic HSCs. Other possible reasons may relate to the differences in human-mouse synteny and the fact that mice are inbred potentially making recombination events more likely. Notwithstanding mouse-human differences in LOH frequencies, our data provide strong evidence that increased mutant *Flt3* and *Ras* gene dosage are important for leukemic transformation/progression.

Finally, in order to investigate their role in *Npm1c* AML, we use CRISPR-Cas9 to disrupt selected genes in Cas9-expressing primary mouse leukemia cells. Using this approach we confirmed the requirement for the *HoxA9/10* functional gene network in *Npm1c* AML maintenance. Interestingly, although it is widely appreciated that overexpression of *Hoxa9* stimulates leukemic transformation^{22,29,33}, in our model disruption of *Hoxa10* has a more detrimental impact on survival, mirroring our recent genome wide essentiality screen in the *NPM1c*-harboring OCI-AML3 cell line.¹¹

Our study describes the first faithful mouse model of the interaction of *Npm1c* with *Nras*-G12D, the preferred form of oncogenic *NRAS* in human AML.² Both *NPM1c* models share a number of salient characteristics, which are imparted by mutant *Npm1*, such as homeobox gene overexpression and increased self-renewal of hemopoietic progenitors. However, we demonstrate that the co-occurrence of *Npm1c/Flt3-ITD* is significantly more leukemogenic and leads to strikingly different

molecular and cellular consequences compared to *Npm1c/Nras-G12D*, providing a mechanistic explanation for the higher frequency and worse prognosis of *NPM1c/FLT3-ITD* AML. Furthermore, through the generation of Cas9-expressing AML models, we also present a versatile approach for the study of genetic interactions in primary mouse leukemias using CRISPR. Whilst our non-Cas9-expressing *Npm1c/Flt3-ITD* model was helpful in recent studies of new anti-AML therapies³¹, these Cas9-expressing models can be utilized to study both genetic and pharmacological interactions in parallel, and also to perform targeted mechanistic studies.

[3966 words]

Acknowledgements

We thank Professor Gary Gilliland for the *Flt3^{ITD}* mouse and Professors Kevin Shannon and Tyler Jacks for the *Nras^{G12D}* mouse. We would also like to thank Mark Dawson for the kind gift of the *MLL-AF9* retroviral construct. OMD, JLC and GSV are funded by a Wellcome Trust Senior Fellowship in Clinical Science (WT095663MA). AM was funded by the Kay Kendall Leukaemia Fund project grant (KKL634). CG was funded by a Bloodwise Clinical Research Training Fellowship. IV is funded by Spanish Ministerio de Economía y Competitividad subprograma Ramón y Cajal. We thank Servicio Santander Supercomputación for their support. GSV is a consultant for and holds stock in Kymab Ltd, and receives an educational grant from Celgene.

Authorship

Contribution: O.M.D., J.L.C., A.M., C.S.G., C.L., P.G. and G.S.V. performed mouse experiments. O.M.D. and G.S.V. analyzed results; P.W. and M.A. performed histopathological analysis of mouse samples; O.M.D., N.C., R.M.A. and M.S. V. performed transcriptome analysis; I.V. performed analysis of next generation sequencing; O.M.D, S.P. and K.T. performed CRISPR-CAS9 experiments; O.M.D. and G.S.V. designed the study. O.M.D. and G.S.V. wrote the paper with the help of R.R., P.W., M.A. and A.B.

Conflict of interest disclosure: GSV is a consultant for and holds stock in Kymab Ltd, and receives an educational grant from Celgene. All other authors declare no competing financial interests.

Correspondence: George Vassiliou, ¹The Wellcome Trust Sanger Institute, Wellcome Trust Genome Campus, Hinxton, Cambridge, CB10 1SA, UK; e-mail: gsv20@sanger.ac.uk.

Figure Legends

Figure 1. Mutant *Npm1* co-operates with *Nras*-G12D and *Flt3*-ITD to enhance myeloid differentiation and enhance progenitor self-renewal.

(A) Schema for *Mx-1 Cre*, *Npm1*^{fllox-cA}, *Nras*^{LSL-G12D} and *Flt3*^{ITD} inter-crosses. (B) *Nras*^{G12D/+} mice show a subtle and *Npm1*^{cA/+}; *Flt3*^{ITD/+} mice a marked increase in white cell count (WCC), compared to wildtype. Splenic sizes were significantly increased in all mutant genotypes except *Npm1*^{cA/+}, with *Npm1*^{cA/+}; *Flt3*^{ITD/+} showing the most striking phenotype. Bone marrow cellularity was increased only in the presence of the *Nras*^{G12D/+} allele. (C) FACS analysis at 4-5 weeks after mutation induction. Gating strategies depicted are from wildtype mice. Significant differences in the stem and progenitor cell compartments of *Nras*^{G12D/+} and *Flt3*^{ITD/+}, but not *Npm1*^{cA/+} single mutant mice, as previously reported. In double mutant mice, the *Npm1*^{cA/+}; *Nras*^{G12D/+} combination was not significantly different to *Nras*^{G12D/+}, in contrast to *Npm1*^{cA/+}; *Flt3*^{ITD/+} which was markedly different to both *Flt3*^{ITD/+} and *Npm1*^{cA/+} single mutants. (D) Using a cell surface phenotype independent of FLT3 staining, we found that CD45+/EPCR+/CD150+/CD48- HSCs were reduced slightly in *Npm1*^{cA/+}; *Nras*^{G12D/+} and markedly in *Npm1*^{cA/+}; *Flt3*^{ITD/+} mice. (E) Summary of hematopoietic effects of *Npm1*^{cA/+}; *Nras*^{G12D/+} and *Npm1*^{cA/+}; *Flt3*^{ITD/+} double mutations in mice. LK, Lin⁻/Kit⁺; LSK, Lin⁻/Sca-1⁺/Kit⁺; CMP, common myeloid progenitor; MEP, megakaryocyte-erythroid progenitor; GMP, granulocyte-monocyte progenitor; MPP, multi-potent progenitor; LMPP, lymphoid primed multi-potent progenitor; CLP, common lymphoid progenitor and HSC, hematopoietic stem cell. (F) Single *Npm1*^{cA/+} and double *Npm1*^{cA/+}; *Nras*^{G12D/+} or *Npm1*^{cA/+}; *Flt3*^{ITD/+} mutant hematopoietic progenitors show increased self-renewal potential in whole bone marrow serial replating assays (n=4-8). Mean ±SEM are plotted. Significant values are reported for one-way analysis of variance (ANOVA, Bonferroni adjusted); (* P<0.05 vs wildtype, ** P<0.01 vs wildtype, *** P<0.001 vs wildtype), (Δ P<0.05 vs *Flt3*^{ITD/+}, ΔΔ P<0.01 vs *Flt3*^{ITD/+}, ΔΔΔ P<0.001 vs *Flt3*^{ITD/+}), (♣ P<0.05 vs *Nras*^{G12D/+}, ♣♣ P<0.01 vs *Nras*^{G12D/+}, ♣♣♣ P<0.001 vs *Nras*^{G12D/+}), († P<0.05 *Npm1*^{cA/+}; *Nras*^{G12D/+} vs *Npm1*^{cA/+}; *Flt3*^{ITD/+}, †† P<0.01 *Npm1*^{cA/+}; *Nras*^{G12D/+} vs *Npm1*^{cA/+}; *Flt3*^{ITD/+}, ††† P<0.001 *Npm1*^{cA/+}; *Nras*^{G12D/+} vs *Npm1*^{cA/+}; *Flt3*^{ITD/+}).

Figure 2. Impact of *Npm1*^{cA/+} on the transcriptome of *Nras*^{G12D/+} and *Flt3*^{ITD/+} mutant hematopoietic progenitors.

(A) Overlap of differentially expressed mRNAs reveals that *Npm1*^{cA/+} has a dramatic impact on Lin-progenitor GEPs when combined with *Flt3*^{ITD/+}, but only a modest impact when combined with *Nras*^{G12D/+}. Nonetheless, the characteristic hallmarks of *Npm1*^{cA/+} are retained in both double mutant progenitors, namely overexpression of *Hoxa* genes and of the homeobox genes *Hopx* and *Nkx2-3* (also seen in single *Npm1*^{cA/+} progenitors). Gene Set Enrichment Analysis reveals enrichment of

differentially expressed genes from these models in human AMLs harboring mutant *NPM1* or *MLL* gene fusions (**B**) Comparison of human *NPM1*-mutant (*NPM1*^c) versus *NPM1*-wildtype (*NPM1*^{WT}) normal karyotype AML (NK-AML) also shows marked overexpression of *HOXA* and *HOXB* genes, as well as of *NKX2.3* raising the possibility that the latter may mediate some of the effect of *NPM1*^c. (**C**) Effects of *Nkx2-3* and *Hoxa9* over-expression on mouse hematopoietic progenitors. (i) Lin⁻ bone marrow progenitors from wildtype and *Flt3*^{ITD/+} mice were transduced with MSCV-*Nkx2.3*-CFP and/or MSCV-*Hoxa9*-GFP constructs, maintained in liquid culture for 7 days, FACS sorted for CFP and GFP single and for double transfected cells and plated in semi-solid media. (ii) Colony assays of 2,500 transduced cells show that both MSCV-*Hoxa9* and MSCV-*Nkx2-3* conferred an increase in self-renewal of both wildtype and *Flt3*^{ITD/+} cells. However, double MSCV-*Hoxa9*/MSCV-*Nkx2-3* transfected cells showed no further changes in self-renewal when compared to MSCV-*Hoxa9* alone. Mean ± SEM (n=3); *p<0.05; **p<0.01; ***p<0.001; students t-test). (**D**) Sorting strategy for LSK/CD34⁺/Flt3⁺/CD48⁺ progenitor cells and overlap of differentially expressed genes (Illumina MouseWG-6 v2 Expression BeadChip) for (i) *Nras*^{G12D/+} vs *Npm1*^{cA/+}; *Nras*^{G12D/+} and (ii) *Flt3*^{ITD/+} vs *Npm1*^{cA/+}; *Flt3*^{ITD/+} MPPs datasets. (**E**) Heat map of normalised *Hox* gene expression in purified (i) MPP and (ii) Lin⁻ populations reveal that *Npm1*^{cA/+} mutants (single or double) have similar patterns of *Hox* gene expression to wildtype (normalised average expression values are used to generate heat map values). (**F**) Differentially expressed genes in *Npm1*^{cA/+}; *Flt3*^{ITD/+} MPPs vs wildtype controls.

Figure 3. *Npm1*^{cA} and *Nras*^{G12D} co-operate to drive high penetrance AML.

(**A**) Kaplan Meier survival curves of wildtype (n=23), *Npm1*^{cA/+} (n=34), *Nras*^{G12D/+} (n=40), *Flt3*^{ITD/+} (n=39), *Npm1*^{cA/+}; *Nras*^{G12D/+} (n=46) and *Npm1*^{cA/+}; *Flt3*^{ITD/+} (n=40). Double mutant (*Npm1*^{cA/+}; *Nras*^{G12D/+} and *Npm1*^{cA/+}; *Flt3*^{ITD/+}) mice had a significantly shortened survival when compared to single mutants, whilst *Npm1*^{cA/+}; *Flt3*^{ITD} had significantly shorter survival than *Npm1*^{cA/+}; *Nras*^{G12D/+} mice. (**B**) Results of independent histopathological analysis of aged moribund mice. Incidence of AML in compound *Npm1*^{cA/+}; *Nras*^{G12D/+} and *Npm1*^{cA/+}; *Flt3*^{ITD/+} mice is increased compared to *Npm1*^{cA/+}, *Nras*^{G12D/+} and *Flt3*^{ITD/+} mice. Examples of complete effacement of splenic tissue and infiltration of myeloid blast cells in liver tissue from *Npm1*^{cA/+}; *Nras*^{G12D/+} and *Npm1*^{cA/+}; *Flt3*^{ITD/+} AMLs are presented. Reduced MPO staining in diseased tissues is observed in samples categorized as AML without maturation (AML-) compared to those categorized as AML with maturation (AML+). H&E, Haematoxylin and eosin; MPO, myeloperoxidase.

Figure 4. Leukemic progression in double mutant mice involves increased *Nras*^{G12D} or *Flt3*^{ITD} allele dosage

(**A**) Increase in *Flt3*^{ITD} allele burden in AMLs from *Npm1*^{cA}; *Flt3*^{ITD} mice through loss of heterozygosity for the locus. (i) *Flt3*^{ITD} amplicon sequencing (MiSeq) of leukemic bone marrow or spleen DNA (FN2-FN7). Tail DNA amplified from 2-week-old *Flt3*^{+/+}, *Flt3*^{ITD/+}, *Flt3*^{ITD/ITD} mice was used as control. (ii) Normalised Log2 ratio plots show copy neutrality of chr5 and the *Flt3* locus in 7/7 *Npm1*^{cA}; *Flt3*^{ITD} murine AMLs (FN-AMLs) tested. (**B**) (i) Summary of aCGH showing copy number gain at the *Nras* locus in AMLs RN6-10. (ii) Allele fractions for *Nras*^{wt} vs *Nras*^{G12D} show that copy number gains in RN6-

10 involved *Nras*^{G12D}, and that an additional 3 cases (RN3-5) show copy-neutral loss-of-heterozygosity. In addition, two more RN AMLs show gains in mutant NRAS when measuring *Nras*^{wt} vs *Nras*^{G12D} allele fractions (aCGH was not performed on these). Results of two *Npm1*^{cA/+} samples are also shown for comparison purposes (N6, N7). (C) Increased gene dosage of *Nras*^{G12D} correlates with increased levels of phosphorylated RAS effectors pERK1/2. FN2,3,4,6,7= *Npm1*^{cA};*Flt3*^{ITD} AML, RN1-14= *Npm1*^{cA/+};*Nras*^{G12D/+} AML.

Figure 5. Somatic mutations in *Npm1*^{cA/+}, *Npm1*^{cA/+}; *Nras*^{G12D/+} and *Npm1*^{cA}; *Flt3*^{ITD} AMLs. (A) Exome sequencing identifies an increased number of somatic nucleotide variants (SNVs) and small indels in *Npm1*^{cA/+}, compared to *Npm1*^{cA/+}; *Nras*^{G12D/+} (RN-AML) and *Npm1*^{cA}; *Flt3*^{ITD} (FN-AML) AML samples. *Npm1*^{cA/+} 6.8±0.9, *Npm1*^{cA/+}; *Nras*^{G12D/+} 3.3±0.5 and *Npm1*^{cA}; *Flt3*^{ITD/+} 2.6±0.7 (mean±SEM) (** p<0.01 vs *Npm1*^{cA/+} one way ANOVA, Bonferroni adjusted). Total AMLs sequenced; *Npm1*^{cA/+} (n=12), *Npm1*^{cA/+}; *Nras*^{G12D/+} (n=14) and *Npm1*^{cA}; *Flt3*^{ITD} (n=7). (B) Summary of SNVs/Indels detected in AMLs from each genotype as indicated. Those in blue are genes mutated in the TCGA AML dataset. Those in red are exact or synonymous mutations detected in the TCGA AML dataset. (C) Co-occurrence of SNVs and CNVs. Depicted are SNVs and focal copy number variations (CNVs) which have been formally detected in the TCGA AML¹⁹ dataset or detected as common insertion sites (CIS) in our previously published *Npm1*^{cA/+} Sleeping Beauty Transposon screen¹⁸. Mutant allele copy gains, chromosome gains and losses depicted. For copy number variation, colour coded boxes are based on log2 ratios (aCGH) and are not representative of CNV size. For a complete overview of all CNV and SNV co-occurrence see Supplemental Figure S6.

Figure 6. *MLL*, *Hox* genes and their partners are required for the survival of *Npm1*^{cA}-driven AML cells. (A) Schematic depicting the derivation and liquid culture of *Rosa26-EF1-Cas9* expressing AML cell lines. CRISPR-EF1-Cas9 based assessment of individual genes aberrantly expressed in *Npm1*^{cA/+}; *Nras*^{G12D/+} and *Npm1*^{cA}; *Flt3*^{ITD} mice. CAS9 activity of these mouse AML cell lines was validated as described previously (Supplementary Figure S7A).¹¹ Individual *Rosa26-EF1-Cas9* expressing cell lines were derived from two mice of each genotype. *In vitro* competitive assays were performed over a 23 day period using AML cell lines transduced with lentivirus expressing gRNAs for the indicated gene, and the BFP-positive fraction compared with the non-transduced population. Results were normalized to day 3 for each gRNA. Results from AML cell lines transduced with guide RNAs targeting Hoxa-related (B) and non-Hoxa related (C) genes. gRNA sequences were selected from a previously published library¹¹ and are detailed in Supplementary Table S15. Guides against the pan essential *Npm1* gene are used as a control.

References

- 529 1. Cancer Genome Atlas Research N, Ley TJ, Miller C, et al. Genomic and epigenomic
530 landscapes of adult de novo acute myeloid leukemia. *N Engl J Med.* 2013;368(22):2059-
531 2074.
- 532 2. Papaemmanuil E, Gerstung M, Bullinger L, et al. Genomic Classification and Prognosis in
533 Acute Myeloid Leukemia. *N Engl J Med.* 2016;374(23):2209-2221.
- 534 3. Falini B, Mecucci C, Tiacci E, et al. Cytoplasmic nucleophosmin in acute myelogenous
535 leukemia with a normal karyotype. *N Engl J Med.* 2005;352(3):254-266.
- 536 4. Welch JS, Ley TJ, Link DC, et al. The origin and evolution of mutations in acute myeloid
537 leukemia. *Cell.* 2012;150(2):264-278.
- 538 5. Lee BH, Tothova Z, Levine RL, et al. FLT3 mutations confer enhanced proliferation and
539 survival properties to multipotent progenitors in a murine model of chronic myelomonocytic
540 leukemia. *Cancer Cell.* 2007;12(4):367-380.
- 541 6. Li Q, Haigis KM, McDaniel A, et al. Hematopoiesis and leukemogenesis in mice expressing
542 oncogenic NrasG12D from the endogenous locus. *Blood.* 2011;117(6):2022-2032.
- 543 7. Vassiliou GS, Cooper JL, Rad R, et al. Mutant nucleophosmin and cooperating pathways drive
544 leukemia initiation and progression in mice. *Nat Genet.* 2011;43(5):470-475.
- 545 8. Mupo A, Celani L, Dovey O, et al. A powerful molecular synergy between mutant
546 Nucleophosmin and Flt3-ITD drives acute myeloid leukemia in mice. *Leukemia.*
547 2013;27(9):1917-1920.
- 548 9. Mallardo M, Caronno A, Pruneri G, et al. NPMc+ and FLT3_ITD mutations cooperate in
549 inducing acute leukaemia in a novel mouse model. *Leukemia.* 2013;27(11):2248-2251.
- 550 10. Sportoletti P, Varasano E, Rossi R, et al. Mouse models of NPM1-mutated acute myeloid
551 leukemia: biological and clinical implications. *Leukemia.* 2015;29(2):269-278.
- 552 11. Tzelepis K, Koike-Yusa H, De Braekeleer E, et al. A CRISPR Dropout Screen Identifies Genetic
553 Vulnerabilities and Therapeutic Targets in Acute Myeloid Leukemia. *Cell Rep.*
554 2016;17(4):1193-1205.
- 555 12. McKerrell T, Park N, Moreno T, et al. Leukemia-associated somatic mutations drive distinct
556 patterns of age-related clonal hemopoiesis. *Cell Rep.* 2015;10(8):1239-1245.
- 557 13. McKerrell T, Moreno T, Ponstingl H, et al. Development and validation of a comprehensive
558 genomic diagnostic tool for myeloid malignancies. *Blood.* 2016;128(1):e1-9.
- 559 14. Li Q, Bohin N, Wen T, et al. Oncogenic Nras has bimodal effects on stem cells that
560 sustainably increase competitiveness. *Nature.* 2013;504(7478):143-147.
- 561 15. Wang J, Kong G, Liu Y, et al. Nras(G12D/+) promotes leukemogenesis by aberrantly
562 regulating hematopoietic stem cell functions. *Blood.* 2013;121(26):5203-5207.
- 563 16. Mead AJ, Kharazi S, Atkinson D, et al. FLT3-ITDs instruct a myeloid differentiation and
564 transformation bias in lymphomyeloid multipotent progenitors. *Cell Rep.* 2013;3(6):1766-
565 1776.
- 566 17. Shih AH, Jiang Y, Meydan C, et al. Mutational cooperativity linked to combinatorial
567 epigenetic gain of function in acute myeloid leukemia. *Cancer Cell.* 2015;27(4):502-515.
- 568 18. Akashi K, Traver D, Miyamoto T, Weissman IL. A clonogenic common myeloid progenitor that
569 gives rise to all myeloid lineages. *Nature.* 2000;404(6774):193-197.
- 570 19. Kent DG, Copley MR, Benz C, et al. Prospective isolation and molecular characterization of
571 hematopoietic stem cells with durable self-renewal potential. *Blood.* 2009;113(25):6342-
572 6350.
- 573 20. Spencer DH, Young MA, Lamprecht TL, et al. Epigenomic analysis of the HOX gene loci
574 reveals mechanisms that may control canonical expression patterns in AML and normal
575 hematopoietic cells. *Leukemia.* 2015;29(6):1279-1289.
- 576 21. Lavalley VP, Baccelli I, Kros J, et al. The transcriptomic landscape and directed chemical
577 interrogation of MLL-rearranged acute myeloid leukemias. *Nat Genet.* 2015;47(9):1030-
578 1037.

- 579 22. Thorsteinsdottir U, Mamo A, Kroon E, et al. Overexpression of the myeloid leukemia-
580 associated Hoxa9 gene in bone marrow cells induces stem cell expansion. *Blood*.
581 2002;99(1):121-129.
- 582 23. Kogan SC, Ward JM, Anver MR, et al. Bethesda proposals for classification of nonlymphoid
583 hematopoietic neoplasms in mice. *Blood*. 2002;100(1):238-245.
- 584 24. Stirewalt DL, Pogossova-Agadjanyan EL, Tsuchiya K, Joaquin J, Meshinchi S. Copy-neutral loss
585 of heterozygosity is prevalent and a late event in the pathogenesis of FLT3/ITD AML. *Blood*
586 *Cancer J*. 2014;4:e208.
- 587 25. Hirata M, Sasaki M, Cairns RA, et al. Mutant IDH is sufficient to initiate enchondromatosis in
588 mice. *Proc Natl Acad Sci U S A*. 2015;112(9):2829-2834.
- 589 26. Weisberg E, Nonami A, Chen Z, et al. Identification of Wee1 as a novel therapeutic target for
590 mutant RAS-driven acute leukemia and other malignancies. *Leukemia*. 2015;29(1):27-37.
- 591 27. Shi J, Wang E, Zuber J, et al. The Polycomb complex PRC2 supports aberrant self-renewal in a
592 mouse model of MLL-AF9;Nras(G12D) acute myeloid leukemia. *Oncogene*. 2013;32(7):930-
593 938.
- 594 28. Danis E, Yamauchi T, Echanique K, et al. Inactivation of Eed impedes MLL-AF9-mediated
595 leukemogenesis through Cdkn2a-dependent and Cdkn2a-independent mechanisms in a
596 murine model. *Exp Hematol*. 2015;43(11):930-935 e936.
- 597 29. Kumar AR, Hudson WA, Chen W, Nishiuchi R, Yao Q, Kersey JH. Hoxa9 influences the
598 phenotype but not the incidence of MLL-AF9 fusion gene leukemia. *Blood*. 2004;103(5):1823-
599 1828.
- 600 30. Dawson MA, Prinjha RK, Dittmann A, et al. Inhibition of BET recruitment to chromatin as an
601 effective treatment for MLL-fusion leukaemia. *Nature*. 2011;478(7370):529-533.
- 602 31. Kuhn MW, Song E, Feng Z, et al. Targeting Chromatin Regulators Inhibits Leukemogenic Gene
603 Expression in NPM1 Mutant Leukemia. *Cancer Discov*. 2016;6(10):1166-1181.
- 604 32. Brumatti G, Salmanidis M, Kok CH, et al. HoxA9 regulated Bcl-2 expression mediates survival
605 of myeloid progenitors and the severity of HoxA9-dependent leukemia. *Oncotarget*.
606 2013;4(11):1933-1947.
- 607 33. Collins CT, Hess JL. Role of HOXA9 in leukemia: dysregulation, cofactors and essential
608 targets. *Oncogene*. 2016;35(9):1090-1098.
- 609 34. Huang Y, Sitwala K, Bronstein J, et al. Identification and characterization of Hoxa9 binding
610 sites in hematopoietic cells. *Blood*. 2012;119(2):388-398.
- 611 35. Dovey OM, Chen B, Mupo A, et al. Identification of a germline F692L drug resistance variant
612 in cis with Flt3-internal tandem duplication in knock-in mice. *Haematologica*.
613 2016;101(8):e328-331.
- 614 36. Choudhary C, Brandts C, Schwable J, et al. Activation mechanisms of STAT5 by oncogenic
615 Flt3-ITD. *Blood*. 2007;110(1):370-374.
- 616 37. Chatterjee A, Ghosh J, Ramdas B, et al. Regulation of Stat5 by FAK and PAK1 in Oncogenic
617 FLT3- and KIT-Driven Leukemogenesis. *Cell Rep*. 2014;9(4):1333-1348.
- 618 38. Garcia-Cuellar MP, Buttner C, Bartenhagen C, Dugas M, Slany RK. Leukemogenic MLL-ENL
619 Fusions Induce Alternative Chromatin States to Drive a Functionally Dichotomous Group of
620 Target Genes. *Cell Rep*. 2016;15(2):310-322.
- 621 39. Xu J, Haigis KM, Firestone AJ, et al. Dominant role of oncogene dosage and absence of tumor
622 suppressor activity in Nras-driven hematopoietic transformation. *Cancer Discov*.
623 2013;3(9):993-1001.

624

Figure 1.

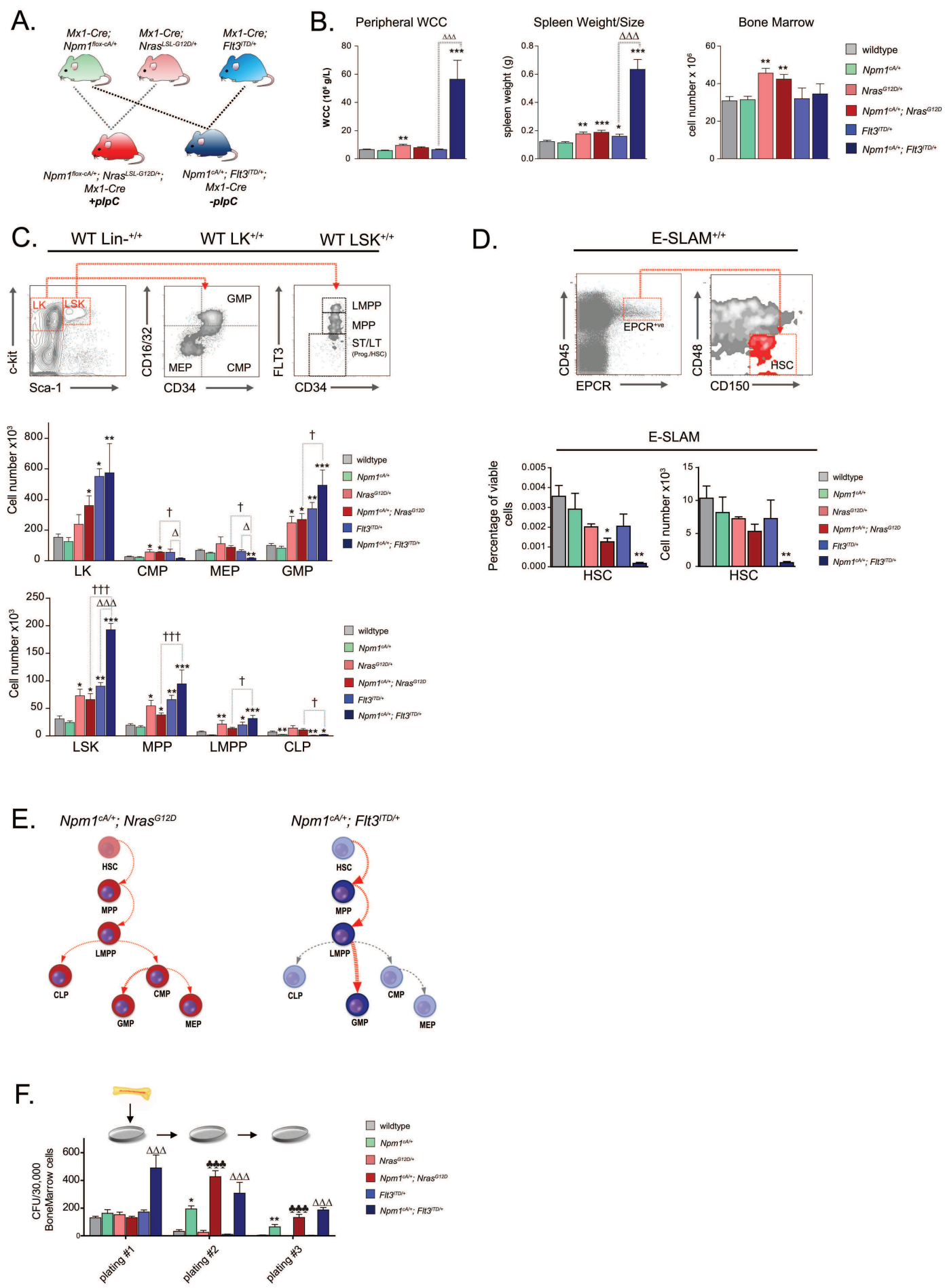


Figure 2

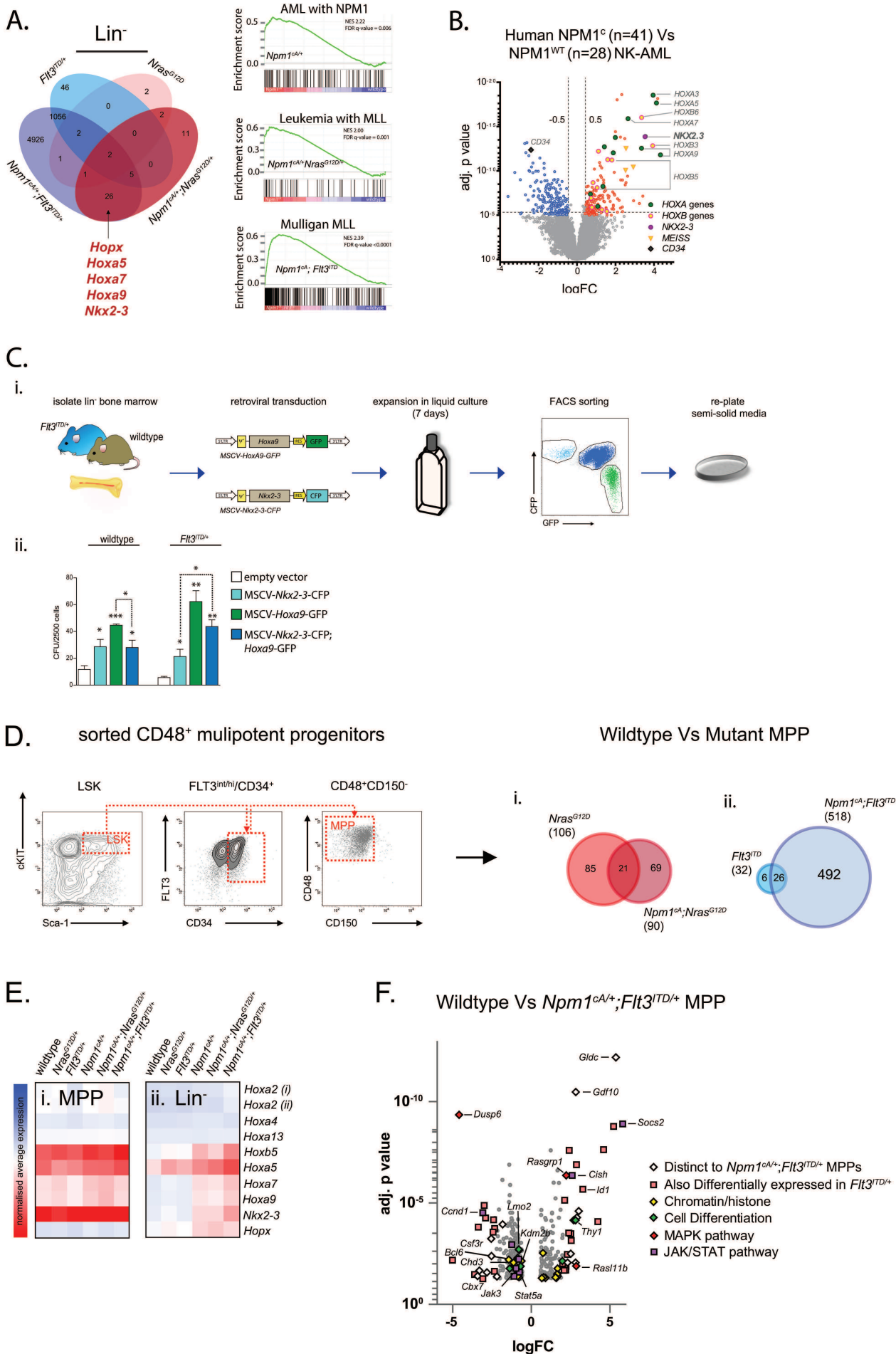
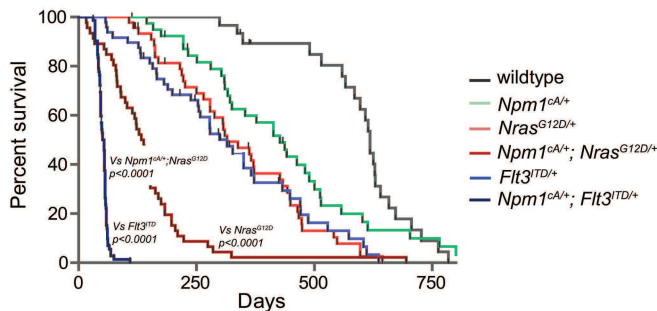


Figure 3

A.



B.

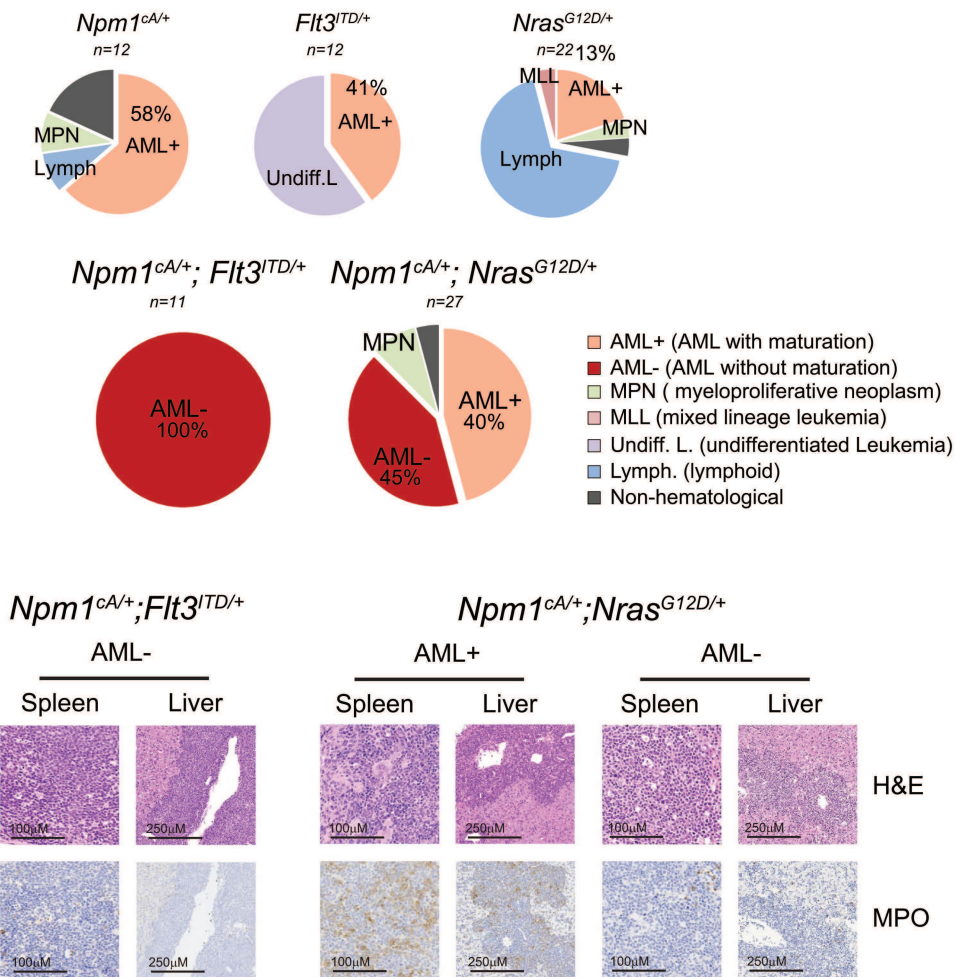
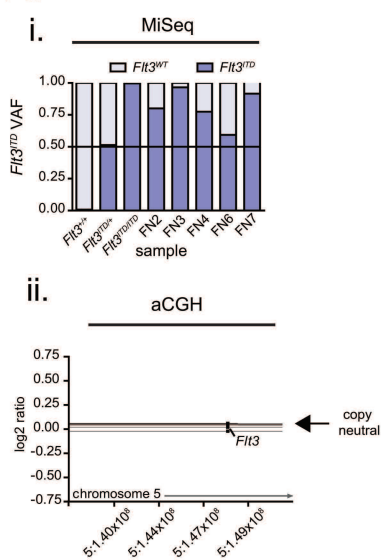
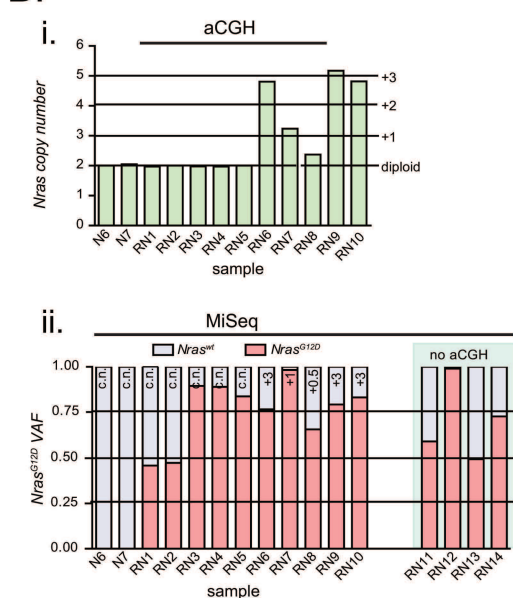


Figure 4

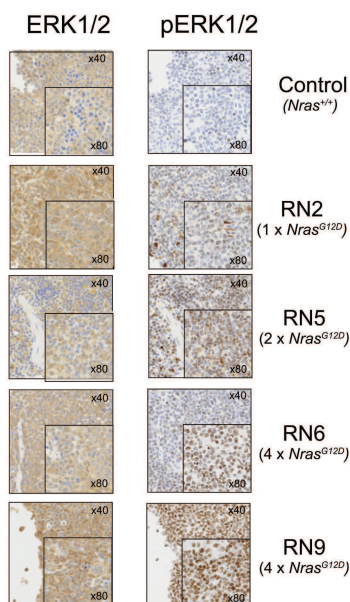
A. *Npm1^{CA}; Flt3^{TD}*



B. *Npm1^{CA/+}; Nras^{G12D/+}*



C. *Npm1^{CA/+}; Nras^{G12D/+}*



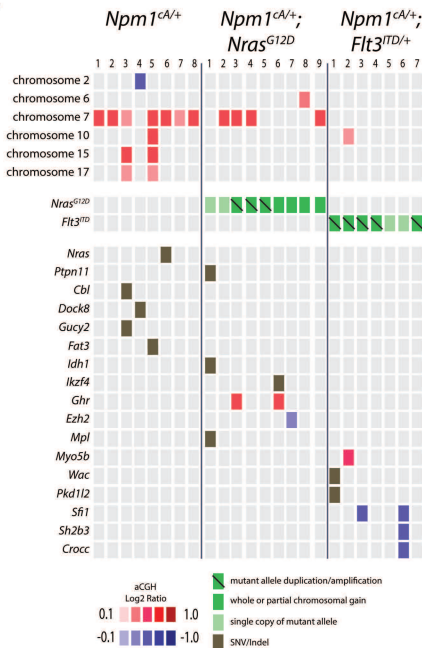
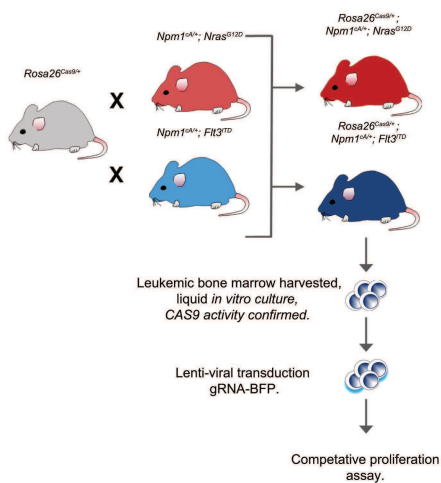
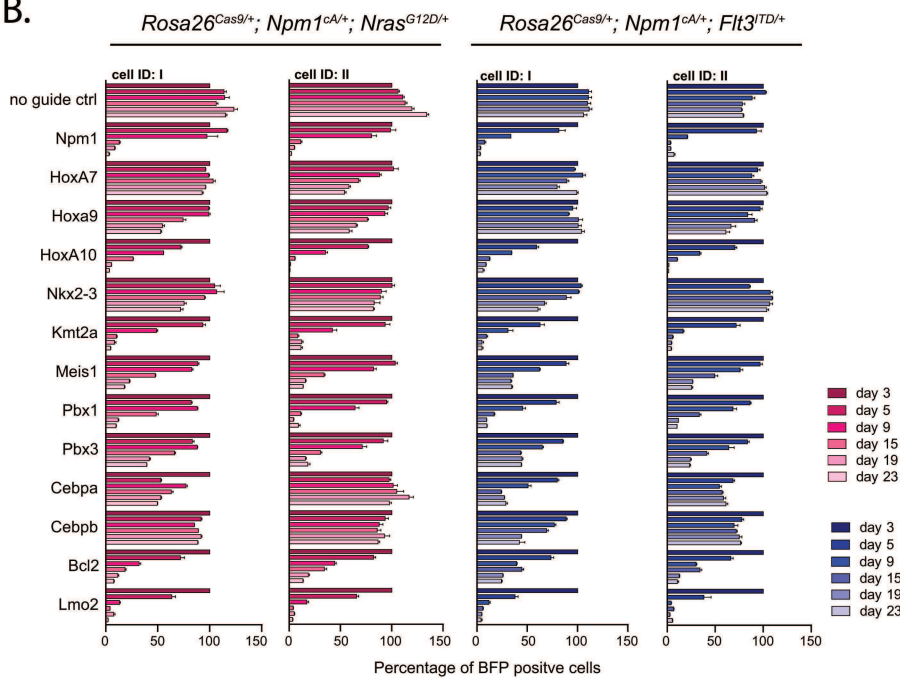
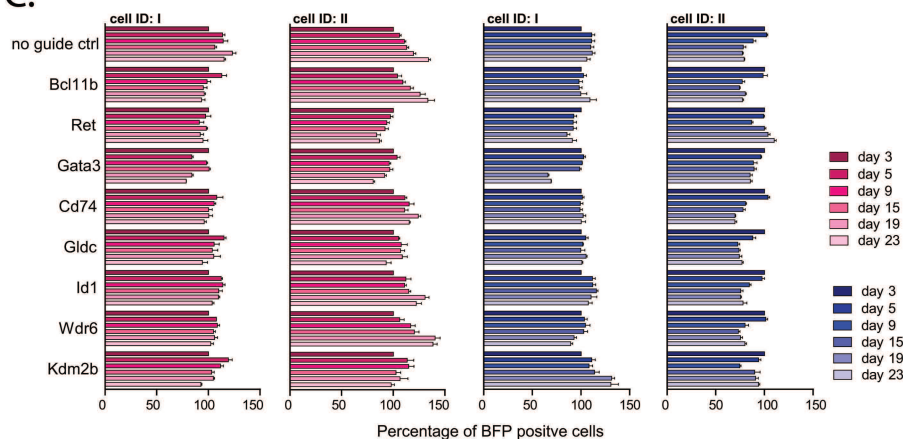


Figure 6**A.****B.****C.**



blood[®]

Prepublished online August 23, 2017;
doi:10.1182/blood-2017-01-760595

Molecular synergy underlies the co-occurrence patterns and phenotype of NPM1-mutant acute myeloid leukemia

Oliver M. Dovey, Jonathan L. Cooper, Annalisa Mupo, Carolyn S. Grove, Claire Lynn, Nathalie Conte, Robert M. Andrews, Suruchi Pacharne, Konstantinos Tzelepis, M.S. Vijayabaskar, Paul Green, Roland Rad, Mark Arends, Penny Wright, Kosuke Yusa, Allan Bradley, Ignacio Varela and George S. Vassiliou

Information about reproducing this article in parts or in its entirety may be found online at:
http://www.bloodjournal.org/site/misc/rights.xhtml#repub_requests

Information about ordering reprints may be found online at:
<http://www.bloodjournal.org/site/misc/rights.xhtml#reprints>

Information about subscriptions and ASH membership may be found online at:
<http://www.bloodjournal.org/site/subscriptions/index.xhtml>

Advance online articles have been peer reviewed and accepted for publication but have not yet appeared in the paper journal (edited, typeset versions may be posted when available prior to final publication). Advance online articles are citable and establish publication priority; they are indexed by PubMed from initial publication. Citations to Advance online articles must include digital object identifier (DOIs) and date of initial publication.